Helium ion beam lithography (HIBL) using HafSOx as the resist

Feixiang Luo*[1, 3], Viacheslav Manichev[1, 3], Mengjun Li[1, 3], Gavin Mitchson[4], Boris Yakshinskiy[2, 3], Torgny Gustafsson[2, 3], David Johnson[4] and Eric Garfunkel[1, 3]

[1]Department of Chemistry and Chemical Biology, [2]Department of Physics and Astronomy, and [3]Rutgers Institute for Advanced Materials, Devices and Nanotechnology, Rutgers University, 610 Taylor Rd, Piscataway, NJ, 08854, USA
[4]Department of Chemistry and Chemical Biology, University of Oregon, Eugene, OR, 97403, USA

ABSTRACT

Helium ion beam lithography (HIBL) is a novel alternative lithographic technique with the capacity of fabricating high-resolution and high-density features. Only limited research has been performed exploring HIBL to date. HafSOx ($Hf(OH)_{4-2x-2y}(O_2)_x(SO_4)_y \cdot qH_2O$) is a negative-tone inorganic resist that is one of several candidate resist materials for extreme ultraviolet lithography (EUVL) and e-beam lithography (EBL), and has been demonstrated to show high resolution, moderate sensitivity and low line-edge roughness (LER) in both EUVL and EBL. To date, no ion beam lithography work on HafSOx has been reported. In this study, we tested HafSOx as an HIBL resist and achieved a high sensitivity compared with EBL with a turn-on dose D_{100} ~ 2-4 μC/cm^2. We obtained sub-10 nm line widths with low LER. A simple Monte Carlo simulation suggests that ionizing excitation accounts for most of the incident He ions' energy loss.

Keywords: HIBL, HafSOx, sensitivity, critical dimension, line-edge roughness, Monte Carlo simulation, secondary electrons

1. INTRODUCTION

Semiconductor lithography, in its attempt to follow Moore's law[1], has proceeded through g-, h- and i-line Hg sources and deep ultraviolet (DUV) excimer lasers (e.g. KrF and ArF). It is now trying to transition to extreme ultraviolet lithography (EUVL)[2]. EUVL offers the promise of significant improvements in critical dimensions (CD) relative to current optical projection techniques, and has become the most exciting technique for next generation lithographies (NGL). Unfortunately, EUVL is still facing challenges including inadequate source power, reflective photomasks issues, optical quality and durability, and resist optimization [3]. Ion beam lithography, especially fast light ions (e.g. protons and helium ions), has received some attention due to its negligible proximity effect [4], attributed to low lateral and back scattering relative to e-beam lithography EBL. Moreover, due to the much larger stopping power of ions [5] compared with light electrons, more energy might be expected to be deposited in the top tens of nanometers of the resist film, which may result in a significant improvement in sensitivity [6]. In 2007, Carl Zeiss SMT released the first commercial scanning helium ion microscope (SHIM) [7] making helium ion beam lithography (HIBL), in addition to SHIM, accessible to general users.

*fl170@scarletmail.rutgers.edu; Phone: +1-848-565-5467

Advances in Patterning Materials and Processes XXXIII, edited by Christoph K. Hohle, Todd R. Younkin,
Proc. of SPIE Vol. 9779, 977928 · © 2016 SPIE · CCC code: 0277-786X/16/$18 · doi: 10.1117/12.2219239

HafSOx was first reported as a solution-processible dielectric layer [8] and was then found to have excellent resist capabilities upon electron or photon exposure. HafSOx works as a resist after adding H_2O_2 in the precursor solution as the radiation sensitivity moiety [9]. Unlike conventional polymer resist films, small HafSOx clusters are the building blocks of the inorganic resists, and have been observed both in the aqueous precursor solution and solid films [10, 11]. The smaller effective "particle" size of the HafSOx resist (relative to polymer resists) may demonstrate higher resolution features and lower pattern edge roughness precisely because the HafSOx can be developed by removing smaller sections of the resist.

In this study, we worked on a Carl Zeiss ORION PLUS SHIM system and investigated the lithographic performance of HafSOx as a resist with HIBL. Moreover, Monte Carlo simulations have been conducted to model the helium ion interaction with the HafSOx film and to compare its behavior with what is observed in the electron beam case.

2. EXPERIMENTAL DETAILS

Precursor solution preparation $HfOCl_2 \cdot 8H_2O$ (98+%, Alfa Aesar) powder was dissolved into 18.2 MΩ deionized water (Millipore) at approximately 1 M concentration followed by filtration to make a hafnium stock solution. TGA (Perkin Elmer TGA7, Thermogravimetric Analyzer) was used to determine the concentration. A portion of a 50 µl hafnium stock solution was placed inside a platinum crucible, which then was sealed in a quartz tube in a flowing oxygen atmosphere. The heating process was programmed into three stages: (i) 90˚C for 150 min, (ii) 500˚C for 30 min, and (iii) 800˚C for 120 min with a heating rate 10 °C/min. The concentration of the stock solution was calculated based on the mass of fully oxidized hafnium dioxide. 1 M H_2SO_4 (Sigma-Aldrich) and 30 wt % H_2O_2 (Sigma-Aldrich) were used as received. The HafSOx precursor solution was prepared by mixing the $HfOCl_2$ stock solution, H_2O_2, and H_2SO_4 solutions, and diluting with 18.2 MΩ Millipore water to a final concentration of approximately 0.15 M. A standard $HfOCl_2$:H_2O_2:H_2SO_4 ratio of 1:3:0.7 was used for all HafSOx films. All HafSOx solutions were made fresh within 1 hour prior to film deposition.

Film deposition For all HafSOx films used for patterning, single-side polished n-type As-doped Si<100> wafers (Resistance 0.001-0.005 ohm-cm) with native oxides were used as the substrate. Prior to the HafSOx deposition, the Si wafers were cleaned by consecutive sonication in acetone, isopropanol (or methanol) and deionized water (18.2 MΩ). Next, the wafers would be treated under an oxygen plasma for 10 mins or by UV/ozone for 15 mins to remove surface adventitious organic carbon and create a surface with a higher –OH termination, helpful in improving wetting of surface for the HafSOx deposition. The 0.15 M precursor solution was filtered by 0.45µm PTFE (Polytetrafluoroethylene) filters then deposited by spin coating (Laurell Technologies) at 3000 rpm for 30s with an acceleration rate of 3000 rpm/s, and finally moved onto a hotplate and soft baked at 80 °C for 3 mins. After cooling down in air, the films were ready for patterning and characterization.

Characterization techniques Rutherford backscattering spectrometry (RBS) was performed using a 2MeV He^{2+} beam source from a 1.7 MV tandem accelerator with an ion current of 2-3 nA. During the RBS measurement, the incident beam was normal to the surface and the backscattered He ions were collected by two silicon surface barrier detectors (at ~100° and ~160° scattering angles for glancing and backscattering). Data fitting and modeling were accomplished using the SIMNRA 6.06 software package. Films were also characterized by atomic force microscopy (AFM) using Park Systems NX-10. Measurements were done in the non-contact mode with a PPP-NCHR tip (Nanosensors, tip radius <10 nm).

Helium ion beam lithography and microscopy A Carl Zeiss ORION PLUS SHIM system, operated at 30 kV, was used for patterning and imaging. The ion beam current was usually kept below 1 pA. For the sensitivity test, 10 nm was selected as the pixel spacing while, for thin line patterns, the pixel spacing was selected in the range of 0.2 nm to 10 nm. After the helium ion exposure, the exposed films were developed in a tetramethylammonium hydroxide solution (TMAH, 25 wt. % in water) for 1 min followed by a 300 °C hard-bake for 5 mins.

Pattern analysis The LER, line width roughness (LWR), and CD were calculated from high-resolution, top-down secondary electron images of sets of five patterned lines acquired using the SHIM and following the methods recommended by the ITRS [12]. The LER was calculated as three times the standard deviation in the line edge position (average from top and bottom line edges), the LWR is calculated as three times the standard deviation in the line width, and the CD is the average line width. The LER, LWR, and CD values were calculated for each line in each set, then averaged to describe the set as a whole. The uncertainty in each measurement comes from the standard deviation of the five average measurements. Due to resolution constraints, approximately 450 nm lengths of each line were used for the calculations. The images were processed using the freely available image processing software ImageJ. The images were smoothed and converted to an 8-bit binary image format such that the patterned lines were completely black (greyscale value 255) and the background was completely white (greyscale value 0). Line widths and line edge positions for each line were determined using 450 nm long rectangular boxes that completely encompassed each line or line edge. The box provided a column-averaged greyscale profile that was then converted to either a width or edge position profile using the height of the box, from which the average width, width standard deviation, and edge position standard deviation could be extracted.

Monte Carlo simulation The commercial software SRIM (the stopping and range of ions in matter) and CASINO V. 2.48[13] (Monte Carlo simulation of electron trajectory in solids) were used to simulate trajectories of helium ions and electrons respectively. Both simulations were performed based on 1000, 30 keV particles using same film model derived from RBS and AFM data. In CASINO (electrons), a 0.1 nm beam size was set to have a comparable beam size with helium ions (atom size beam as default) simulated in SRIM.

3. RESULTS AND DISCUSSION

3.1 HafSOx resist sensitivity test with HIBL and EBL

Resist sensitivity was explored with 30 keV helium ions and compared to electronics at the same energy; their contrast curves are shown in Figure 1(a). In the case of 30 keV helium ions, D_{100} (the dose at which the developed features start to have 100% of as-deposit resist thickness) occurs at approximately 4 $\mu C/cm^2$. In comparison with 30 keV electrons (D_{100} = 420 $\mu C/cm^2$), the helium ions exhibit ~100 times higher sensitivity. This has been reported in other resist systems as well [6, 14]. Considering the drastic difference in stopping power between helium ions and electrons, we think the stopping power, most of which occurs from secondary electron generation to activate the resist films, is the main contributor to the significant sensitivity improvement. Though the specific stopping power data of 30 keV He^+ ions interacting with HafSOx has not been reported, we summarized of stopping power ratios of He^{2+} ions to e^- in various organic and inorganic materials [5]. As shown in Figure 1(b) for a list of common material, the helium ion to electron stopping power ratio are in the 50-100 range among tested resists [6] are in agreement with our results of a 50-100 times sensitivity improvement.

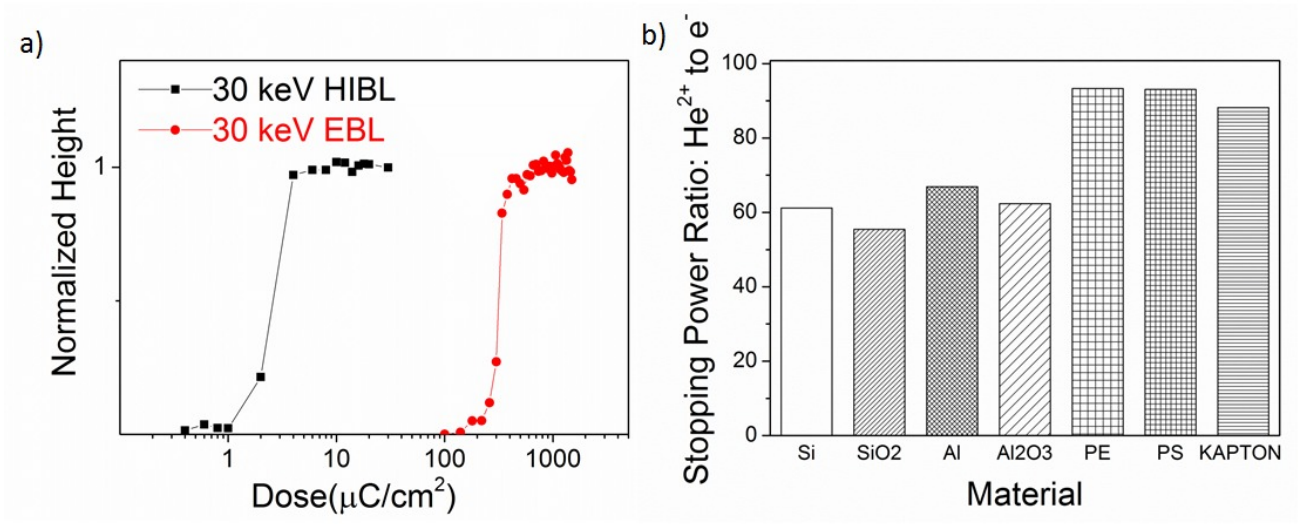

Figure 1(a) The contrast curve comparison between HIBL and EBL with a 30 kV acceleration voltage, and (b) the stopping power ratio between He^{2+} and e^- in a few common materials[5].

Due to the limited availability of helium ion patterning, only a few resists have been tested with HIBL and we summarized their reported sensitivity data, in terms of D_{50}, in Table 1 and compared their results with the best sensitivity we have achieved on HafSOx resists. Surprisingly, we found that HafSOx outperformed most common resists with regard to sensitivity and almost shares the best sensitivity with CAR, though, in the EBL case, HafSOx is not quite as good as CAR.

Resist	Tone	Sensitivity ($^*D_{50}$, μC/cm^2)
PMMA	Negative	68[6]
PMMA	Positive	2[6]
HSQ	Negative	1.7[6], 31[14]
CAR	Positive	0.93[15]
HafSOx	Negative	**1.0

Table 1 Resists sensitivity comparison using helium ion beam as incident particles. Acronyms: poly (methyl methacrylate) = PMMA; hydrogen silsesquioxane = HSQ; chemically amplified resist = CAR

*D_{50} is defined as the dose at which the developed features have half of the thickness of the original resist (positive tone) or of a fully-exposed and developed resist (negative tone).

** The best sensitivity we have achieved.

3.2 Study of CD and LER on HafSOx resist

Following the sensitivity investigation, resolution tests of HafSOx with HIBL were conducted by making line patterns with various input line widths at various doses. In particular, the effective line width value we input into the patterning software was controlled in part by changing the value of pixel spacing and the number of single-pixel-wide lines. Figure 2(a) is a SHIM image of a line-pattern example exhibiting one of the smallest average line width (9.3 nm) and LER (2.9 nm, 3σ) values we achieved at the dose of 40 μC/cm^2 with 2 nm as the nominal input line width.

We present data in Figures 2(b) and 2(c) that explore the dependence of average line width and LER on doses and input line width. As shown in Figure 2(b), for all cases, the measured line widths were always larger than the original input values at high doses and tended to reduce when doses were lowered. For some cases (e.g. 20 nm input width), the measured line width does reach the initial input value. However, for smaller desired features (e.g. 2 nm and 5 nm input widths), the measured line width can only be lowered to ~9-10 nm (under our currently explored system and conditions) by lowering the dose. Further dose reduction leads to intermittent "dot" features. To achieve patterns with line width less than 9 nm, we plan to focus on the optimization of resist properties (such as film thickness and composition) and development chemistries, instead of merely changing exposure parameters.

As shown in Figure 2(c), we find a larger LER is observed at a larger dose in the tested dose region, which is different from some reported simulation and experimental results [16, 17] (using EBL and EUVL). However, considering the very low turn-on dose (D_{100}, ~ 4μC/cm^2), the doses in the tested region all have more than sufficient ion flux. As reported[18], we think the excess helium ions may form helium bubbles near the surface, leading to a higher LER at high ion dose. Irradiation doses below 10 μC/cm^2 are beyond the capability of the current patterning software.

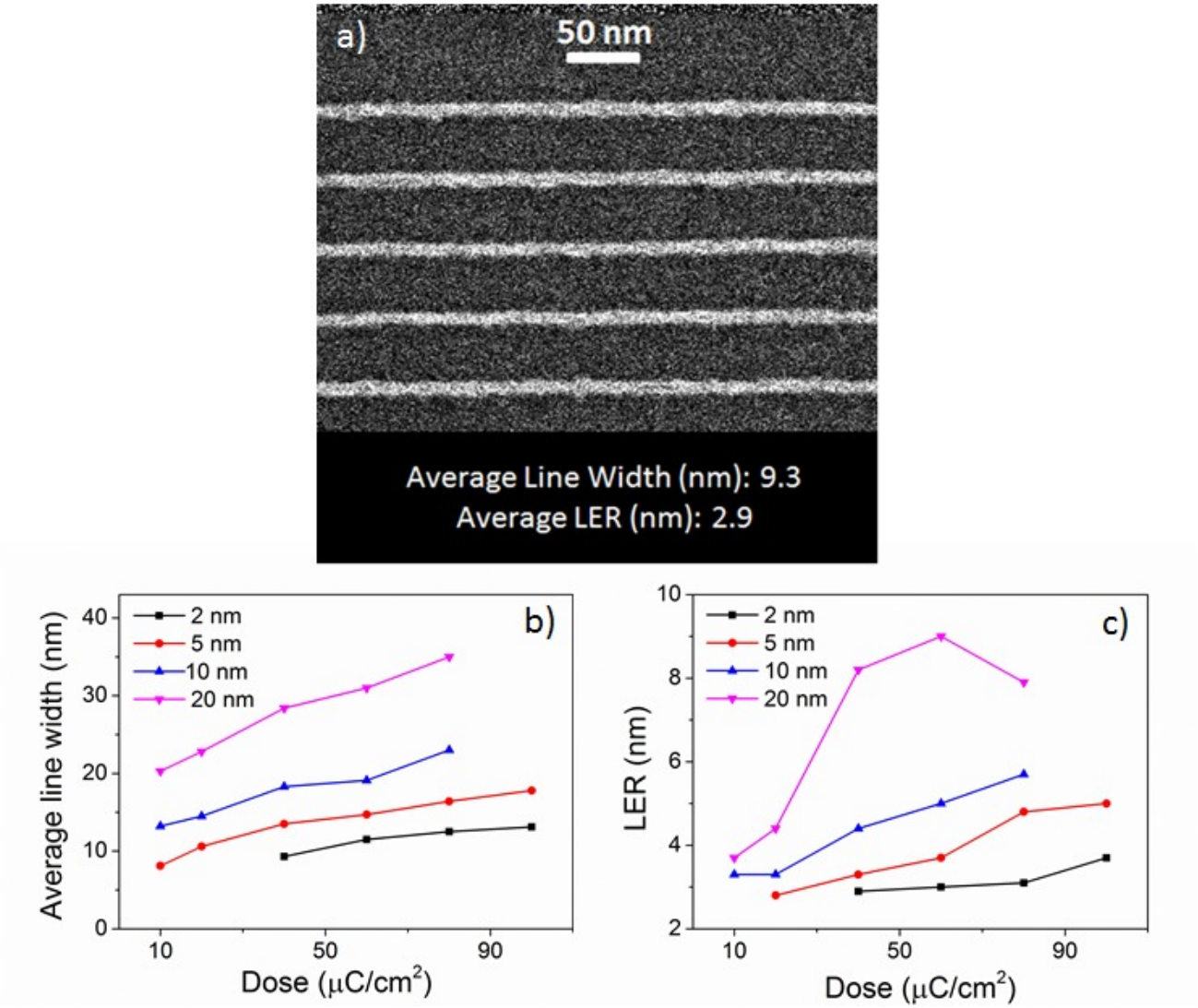

Figure 2 (a) A line pattern showing below-10 nm average line width and LER (3σ) 2.9 nm and the dependence of (b) average line width and (c) LER on doses. 2, 5, 10, 20 nm are the input line width values we set in the software during exposure, not the measured real line widths.

4. RESULTS AND DISCUSSION ON SIMULATION

4.1 Simulation model construction with Rutherford backscattering spectrometry (RBS)

An accurate model of film composition and thickness is central to understanding the system. In order to figure out the film composition and structure, RBS was employed. Figure 3 (a) presents the RBS spectrum of an as-deposited HafSOx film, from which Hf, S, O, C can be distinguished in the form of sharp peaks, while the plateau stands for Si. Considering the low sensitivity of RBS for low Z elements (e.g. O and C), we also conducted x-ray photoelectron spectroscopy (XPS) to better estimate the composition in the surface region. Based on the areal density results obtained by fitting the RBS spectrum, and the thickness of the top HafSOx (21.1 nm) layer from an AFM measurement, a 3-layer film structure was generated, as shown in Figure 3(b). On top of the Si substrate is a silicon oxide layer (~ 13.8 nm, calculated based on the known density of 2.196 g/cm^3 for amorphous silicon dioxide) with a trace amount of inter-diffused Hf and S. The HafSOx film had an approximate composition of $Hf_{0.16}O_{0.58}S_{0.10}C_{0.16}$, situated on the surface of silicon oxide layer with a calculated HafSOx film density of 2.74 g/cm^3.

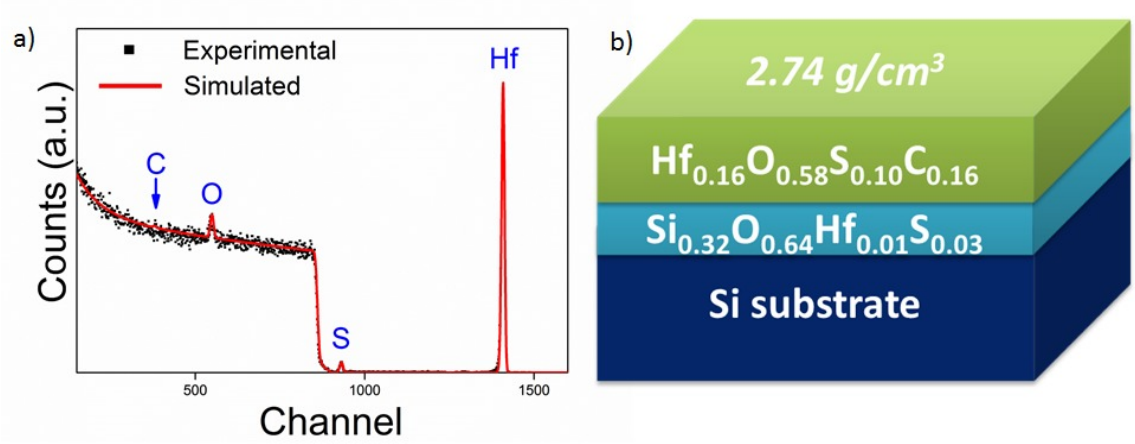

Figure 3 (a) a RBS spectrum of as-deposited HafSOx films including both experimental data and the simulated curve, and (b) a 3-layer film model derived from it. The top layer density was calculated based on areal density data (RBS) and thickness data (AFM).

4.2 Monte Carlo simulation of helium ions and electrons in HafSOx films

Secondary electron activation has been widely reported [15, 19, 20] to be responsible for the radiation induced transformation of resists. Helium ions at 30 keV have also been observed [21] to produce secondary electrons with maximum intensity (based on electron emission data) of between 1-5 eV, with an exponential decay in intensity at higher energies. In this study, we first ran SRIM simulation, based on the film model setup in RBS, to study the energy loss of helium ions in HafSOx. We found ionization, which would further initiate the production of electrons, accounts for more than 93% of the total energy loss. Figure 4(a) shows the energy loss, attributed to ionization, through the three-layer structure of a HafSOx sample for one 30 keV helium ion. In the top HafSOx layer, the average energy loss is around 6 eV/angstrom spotted from the figure. Therefore, the total energy loss happened in the 211 angstrom HafSOx equals 1.27 keV. Based on the above discussion, assuming 5 eV as the average energy of the secondary electrons activating the resist film, we would get a number of 253 secondary electrons produced by one 30 keV helium ion in HafSOx layer. Moreover, considering the average fully activation dose D_{100} = 4 μC/cm^2, which is 0.26 ions/nm^2, it leads to a number of 66 secondary electrons/nm^2 to fully activate the HafSOx resist.

On the other hand, comparing the trajectories of helium ions and electrons, as shown in Figure 4(b), helps us understand the experimental limits and potentials during the exposure process. With the similar starting beam diameter without considering the possible instrumental constraints, we found in the thin (~ 20 nm) HafSOx layer, the electron and helium ion exhibit similar well-confined trajectories, though helium ions have been observed and reported [22] to have much less lateral scattering than the electrons on a much larger scale (e.g. hundreds of nanometers or μm).

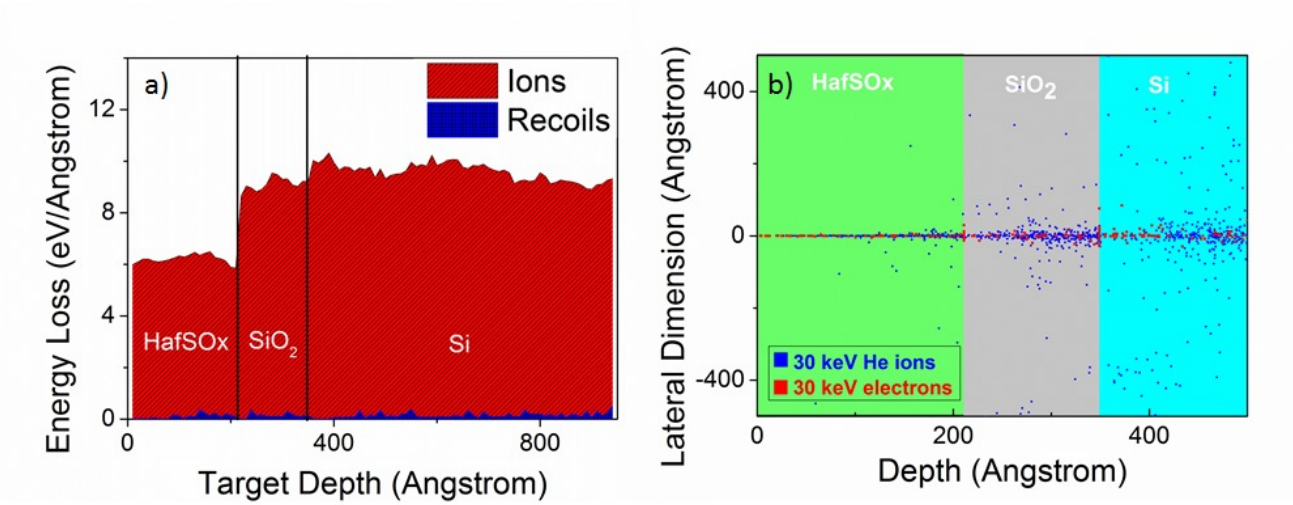

Figure 4 (a) the simulation result of energy loss, due to ionization, inside the HafSOx film and its substrate; (b) The trajectory comparison between He ion and electron at 30 keV.

CONCLUSION

In this study, we investigated the lithographical performance of the novel inorganic HafSOx resist with HIBL and demonstrated its ultra-high sensitivity (D_{100} < 4 μC/cm^2) and a nearly 100 fold increase in sensitivity compared with EBL under the same conditions. Among tested materials, HafSOx, in the best case, exhibits a sensitivity as good as CAR with HIBL. Sub-10 nm line patterns were achieved with low LER in these initial studies. A Monte Carlo simulation of helium ions has been conducted to investigate the energy loss and consecutive secondary electron production in HafSOx film and its comparison with electrons show similarities in trajectories in the top thin HafSOx region.

ACKNOWLEDGEMENTS

The authors gratefully acknowledge the support of the National Science Foundation via the Center for Sustainable Materials Chemistry (an NSF-Center for Chemical Innovation), under Grant CHE-1102637. V.M. and T.G. acknowledge the support from NSF grants DMR MRI 1126468 and DMR1106070. We thank Leonard Feldman (Rutgers) and Douglas Keszler (OSU) for insightful discussion and constructive suggestions.

REFERENCES

[1] Moore, G. E., "Cramming more components onto integrated circuits (Reprinted from Electronics, pg 114-117, April 19, 1965)," Proceedings of the IEEE, 86(1), 82-85 (1998).

[2] Blumenstock, G. M., Meinert, C., Farrar, N. R. *et al.*, "Evolution of light source technology to support immersion and EUV lithography," Advanced Microlithography Technologies, 5645, 188-195 (2005).

[3] Wua, B. Q., and Kumar, A., "Extreme ultraviolet lithography: A review," Journal of Vacuum Science & Technology B, 25(6), 1743-1761 (2007).

[4] Watt, F., Bettiol, A., Van Kan, J. *et al.*, "Ion beam lithography and nanofabrication: a review," International Journal of Nanoscience, 4(03), 269-286 (2005).

[5] Berger, M. J., Coursey, J., Zucker, M. *et al.*, [Stopping-power and range tables for electrons, protons, and helium ions].

[6] van der Drift, E., and Maas, D. J., [Helium ion lithography] Springer, (2012).
[7] Release, C. Z. S. P., [Carl Zeiss SMT Ships World's First ORION Helium Ion Microscope to U.S. National Institute of Standards and Technology], (2008).
[8] Anderson, J. T., Munsee, C. L., Hung, C. M. *et al.*, "Solution-processed HafSOx and ZircSOx inorganic thin-film dielectrics and nanolaminates," Advanced Functional Materials, 17(13), 2117-2124 (2007).
[9] Oleksak, R. P., Ruther, R. E., Luo, F. X. *et al.*, "Chemical and Structural Investigation of High-Resolution Patterning with HafSOx," Acs Applied Materials & Interfaces, 6(4), 2917-2921 (2014).
[10] Oleksak, R. P., and Herman, G. S., "Characterization of high-resolution HafSOx inorganic resists," Extreme Ultraviolet (EUV) Lithography V, 9048, (2014).
[11] Jackson, M. N., Kamunde-Devonish, M. K., Hammann, B. A. *et al.*, "An overview of selected current approaches to the characterization of aqueous inorganic clusters," Dalton Transactions, 44(39), 16982-17006 (2015).
[12] ITRS, "Metrology," (2009).
[13] Drouin, D., Couture, A. R., Joly, D. *et al.*, "CASINO V2.42 - A fast and easy-to-use modeling tool for scanning electron microscopy and microanalysis users," Scanning, 29(3), 92-101 (2007).
[14] Sidorkin, V., van Veldhoven, E., van der Drift, E. *et al.*, "Sub-10-nm nanolithography with a scanning helium beam," Journal of Vacuum Science & Technology B, 27(4), L18-L20 (2009).
[15] Maas, D., van Veldhoven, E., van Langen-Suurling, A. *et al.*, "Evaluation of EUV resist performance below 20-nm CD using helium ion lithography," Extreme Ultraviolet (EUV) Lithography V, 9048, (2014).
[16] Mojarad, N., Gobrecht, J., and Ekinci, Y., "Beyond EUV lithography: a comparative study of efficient photoresists' performance," Scientific Reports, 5, (2015).
[17] Saeki, A., Kozawa, T., Tagawa, S. *et al.*, "Exposure dose dependence on line edge roughness of a latent image in electron beam/extreme ultraviolet lithographies studied by Monte Carlo technique," Journal of Micro-Nanolithography Mems and Moems, 6(4), (2007).
[18] Livengood, R., Tan, S., Greenzweig, Y. *et al.*, "Subsurface damage from helium ions as a function of dose, beam energy, and dose rate," Journal of Vacuum Science & Technology B, 27(6), 3244-3249 (2009).
[19] Jeyakumar, A., [Development of Inorganic Resists for Electron Beam Lithography: Novel Materials and Simulations] Georgia Institute of Technology, (2004).
[20] Kozawa, T., and Tagawa, S., "Radiation Chemistry in Chemically Amplified Resists," Japanese Journal of Applied Physics, 49(3), (2010).
[21] Petrov, Y., and Vyvenko, O., "Secondary electron emission spectra and energy selective imaging in helium ion microscope," Scanning Microscopies 2011: Advanced Microscopy Technologies for Defense, Homeland Security, Forensic, Life, Environmental, and Industrial Sciences, 8036, (2011).
[22] Cohen-Tanugi, D., and Yao, N., "Superior imaging resolution in scanning helium-ion microscopy: A look at beam-sample interactions," Journal of Applied Physics, 104(6), (2008).